Experimental Evaluation of Optical Feedback for Nanopositioning of Piezo Actuator Stage

Piotr Skupin, Mieczyslaw Metzger, Dariusz Choinski
Faculty of Automatic Control, Electronics and Informatics
Silesian University of Technology
Gliwice, Poland
{piotr.skupin, mieczyslaw.metzger, dariusz.choinski}@polsl.pl

***Abstract*—The paper presents the realization of the nanopositioning control of activated sludge samples observed under the microscope. To achieve the desired control goals, the most typical and cheapest components of the positioning system were used. It has been shown both experimentally and numerically that one of the simplest control algorithms (in this case the PI controller) can provide satisfactory good results in positioning control systems. Moreover, based on the simplified description of the microactuator, analytical stability conditions of the closed-loop system have been given. Then, it was possible to find the analytical and experimental stability regions on the controller parameter plane and to compare them against each other.**

Keywords-microactuator; nanopositioning control; hysteresis; stability analysis

I. INTRODUCTION

Nanopositioning control is a very essential issue in various fields of science and technology [1], [2]. A basic device, which allows for very precise and accurate positioning is a piezoelectric actuator (microactuator) using piezoceramic element that undergoes the phenomenon of reverse piezoelectric effect. In most cases, the typical operating range for positioning purposes is 20 to 30 micrometers, and depending on the accuracy of the position measurement, the device allows for positioning with accuracy within a several nanometers. Hence, the piezoceramic actuators are often used in the positioning control of mirrors on the optical table, in microscopes, digital cameras, etc.

Among the many areas, in which microactuators are widely used, broadly defined biotechnology offers a strong application potential of such devices and the typical example is the in-vitro fertilization. The second important field of application of microactuators is the precise positioning of mechanical parts in the laboratory equipment used for a proper conduction of micro-scale processes. In our case, we will focus on the design of positioning control system, which can be used for precise positioning of samples of activated sludge observed under the microscope. However, the key issue in the design of the positioning control system is to provide a precise and accurate measurement of the microactuator stage position.

An interesting paper addressing this problem is the survey paper by Fleming published in Sensors & Actuators A: Physical [3]. This paper describes and compares the following sensors: piezoelectric and piezoresistive strain sensors, resistive and capacitive sensors, electrothermal sensors, eddy current sensors, linear variable displacement transformers, interferometers and linear encoders. The quick reference on the sensors used for nanopositioning control in biotechnology can be found in [4].

In the literature, laser sensors are the most frequently described sensors for nanopositioning purposes (see, e.g., [5-9]). In turn, the application of optical encoder for delay-varying repetitive control of walking piezoactuator can be found in [10]. In [11], the strain gauge sensor was used for hysteresis analysis of the piezostack actuator. These studies were performed for displacements in the range of several micrometers. In turn, the induction coil sensor can be used for positioning in the micro- (but not nano-) scale [12].

In principle, for microscopic observations, it is more convenient to use the same microscope to measure the position of the microactuator stage. Moreover, the microscope can also be used for calibration of position sensors for microactuators, because it can provide a sufficiently high precision in position determination during microscopic observations. More precise positioning is hardly observable be the experimenter, hence, in many cases is not necessary. The application of microscope for positioning control is also described in the literature. For instance, in in-vitro fertilization, two coaxial microactuator stages are used for appropriate positioning of the needle observed under the microscope [13]. This paper also gives a short survey of various positioning sensors used in the in-vitro fertilization equipment. In turn, the paper [14] describes the application of microscope to provide visual feedback in positioning control on the XY plane. It should be emphasized that some papers describing advanced control algorithms (see, e.g., [15], [16]), provide only limited information on the position sensor or measurement technique. Probably, their authors were mainly focused on the presentation of their results assuming that the position measurements are precise and accurate; hence, the measurement errors are negligible.

But, the main reason for which nanopositioning is an interesting control problem is the nonlinear nature of the plant (microactuator), which manifests itself as hysteresis in the relation between position of the microactuator stage and

 ISBN: 978-1-61208-303-2

the control voltage. As a result, it is necessary to implement closed-loop control system, for which accuracy and precision of positioning is only dependent on the applied measurement sensor. Although the application of microscope is an expensive and complex solution (image processing is required), only the image from microscope can provide an accurate position of the microactuator stage. On the other hand, other types of sensors provide indirect information on the actual position of the microactuator stage.

Among the papers dealing with the influence of hysteresis on the quality of positioning control, it is worth mentioning earlier studies (e.g., [17], [18]), which describe piezoelectric actuators. It should be emphasized that the general properties of the closed-loop control systems (e.g., stability or quality of transients) for plants with hysteresis nonlinearity, have been well-known in the field of control theory since the 1950s of the past century. In majority of papers concerning nanopositioning control problem, the hysteresis phenomenon is often taken into account. For instance, the latest attempts to model the hysteresis behavior can be found in [4], [11], [19] and [20].

Among various control algorithms that can be used for positioning purposes, the simplest and historically the first is the classical PI (or PID) control algorithm. These algorithms are frequently applied in the combination with feedforward [13], fuzzy logic [15] or artificial neural networks [21]. The last cited paper [21] describes sliding mode control (SMC) algorithm showing its advantages over the classical PID controller. But, the improvement of the control quality achieved for the SMC is insignificant in comparison to the results for the PID controller. Hence, it leads us to the conclusion that the simple PID algorithm is the better option. For instance, the in-vitro fertilization system described in [13] uses two piezoactuators controlled by two independent PID controllers. Moreover, many authors consider the piezostack actuator to be an interesting nonlinear plant, which can serve as a benchmark system for testing new control algorithms. At this point, it is worth mentioning the advanced delay-varying repetitive control (DVRC) [10] or repetitive control algorithm with feedforward [16].

In this paper, we present an experimental set-up for analysis and calibration of piezostack actuators. The optical microscope is used to obtain the direct measurement of position of the microactuator stage. We will show that the classical PI controller is sufficient to obtain the acceptable control quality. The remainder of the paper is organized as follows. Section II provides details on the laboratory setup and describes a way to obtain information on the stage position, which is then used to manipulate the activated sludge samples during microscopic observations. Section III describes the control algorithm, which is based on the optical feedback provided by the microscope. Finally, Section IV discusses the main results.

II. EXPERIMENTAL SET-UP FOR NANOPOSITIONING CONTROL

The general schema of the measurement set-up is shown in Fig. 1. The presented system uses the microactuator, which allows for positioning in the range up to 25 micrometers, with an accuracy of several nanometers. In order to measure a position of the movable stage of the microactuator, the digital camera coupled with the optical microscope is used.

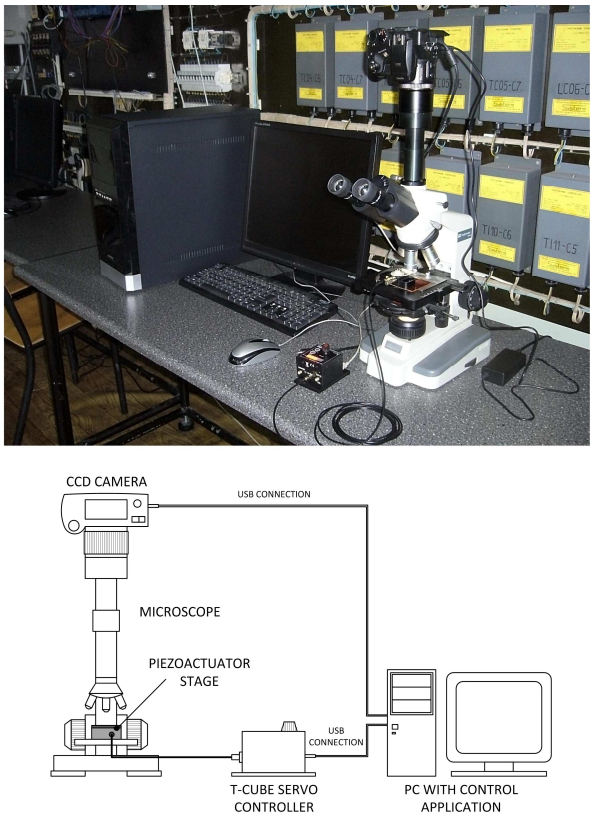

Figure 1. The general scheme of the experimental set-up.

Fig. 2 explains how to receive information on the stage position. A small glass plate, on which the analyzed sample is placed, has been mounted to the microactuator stage. But, to measure the stage position, a piece of tape has been attached to the top surface of the glass plate. This piece of tape is a graphical indicator used to determine the stage position with reference to the microscope stage. The shape of the indicator should be sufficiently large to obtain the stage position in the whole range of displacement and sufficiently small to maximize the field of view during microscopic observations. Then, the microscopic image of 320x240 pixels is recorded by the digital camera and sent to the computer via USB port. In the control application, created in LabVIEW environment, the captured image is processed by the threshold image segmentation method, which is performed on-line. As a result, a 320x240 matrix corresponding to the processed image is filled with ones and zeros. Because, the range of displacement is 25 micrometers, which is equal to 88 pixels, hence, one pixel corresponds to about 284 nanometers for total magnification of 400x (40x objective and 10x ocular). Since the diameter of a single sludge flock varies between 10 and 100 micrometers, the accuracy to 284 nanometers is sufficient for our purposes.

 ISBN: 978-1-61208-303-2

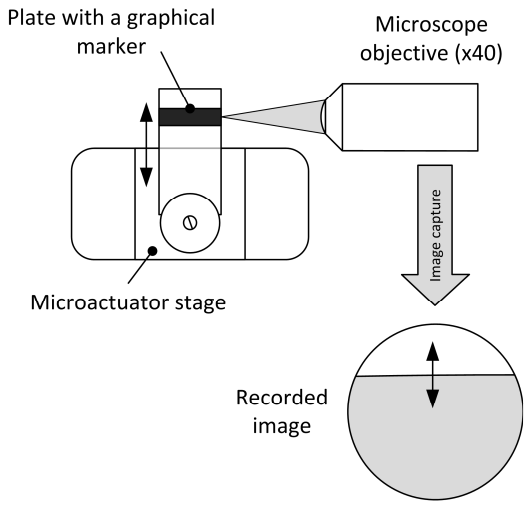

Figure 2. The idea of position measurement of the microactuator stage.

Information on the stage position can be then used by any control algorithm responsible for precise positioning of the microactuator stage. In turn, a single-channel T-Cube servo controller connected to the computer via USB port provides a source of control voltage. The control voltage (0-75[V]) changes the position of the microactuator stage and it can be generated either manually, i.e., in the T-Cube servo controller or indirectly in the control application, which is based on ActiveX components. The possibility of using ActiveX components facilitates the control system design process, which is described in the next section.

III. DESIGN OF POSITION CONTROLLER

Determination and analysis of the static characteristics of the controlled plant (microactuator) is a very important stage in the controller designing process. In the considered case, the static characteristics presents the relation between the stage position in micrometers and the input voltage. These characteristics were obtained by cyclic changes of the input voltage in steps of 2 volts. The obtained characteristics are shown in Fig. 3. Irrespective of the range of input voltage, a hysteresis effect was observed. The hysteresis is a typical phenomenon for piezoceramic materials and it is also noticeable in Fig. 4, which shows the step responses of microactuator stage. The analysis of these responses will help us to determine the dynamical properties of the controlled plant. It can be easily noticed that the same levels of the input voltage correspond to different stage positions. Moreover, the step changes in the input voltage cause instantaneous changes in the microactuator stage position (Fig. 4). Because, in our case, the microactuator stage will be applied for positioning of samples under the microscope, hence, at sampling rate of 10Hz (the sample time T=100[ms]), the much faster dynamics of the microactuator is negligible. In other words, it is assumed that the microactuator is a static element and can be described by the following equation:

$$y = k \cdot u \quad (1)$$

where: y – is the position of the microactuator stage in [μm], u – is the input voltage [V], k=1/3 [μm/V] – is the gain of the plant. It also means that the dynamical properties of the closed-loop system will be entirely determined by the dynamics of the controller. In other situations, it may prove necessary to take into account the dynamical properties of the controlled plant (microactuator system), especially, when the input voltage changes at high frequency. Unfortunately, due to the time needed to process the captured image, it was not possible to set the sample time less than 100 milliseconds. Hence, it was not possible to analyze the behavior of the microactuator stage immediately after the step change in the control voltage. It is worth noting that the problem of control of a static system (without dynamics) is rare and untypical, but can be quite complex, especially when the controlled plant is highly nonlinear.

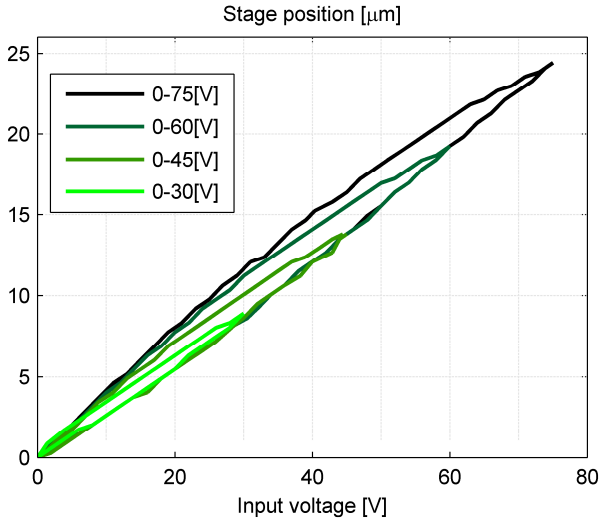

Figure 3. Static characteristics of the controlled plant.

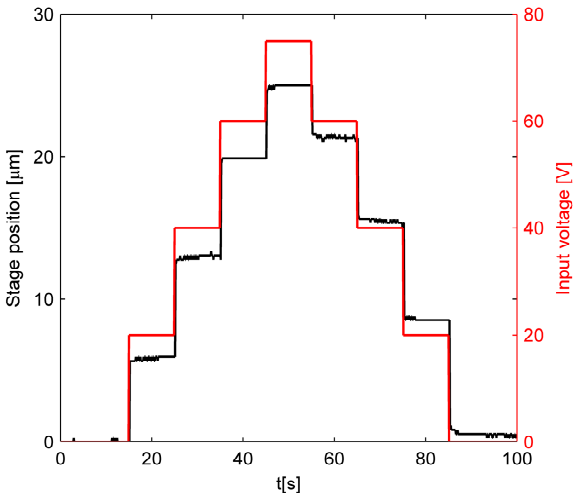

Figure 4. Step responses (black) to step changes in input voltage (red).

 ISBN: 978-1-61208-303-2

The simplified model of the microactuator (1) does not also include the hysteresis behavior, but it will simplify the controller design process. However, to take into account the hysteresis effect, a well-known Preisach model [22], [23] can be applied. Other models proposed in the literature are based, for instance, on artificial neural networks [24].

For positioning purposes, the classical PID controller can be used and its transfer function is as follows:

$$K(s) = k_p\left(1+\frac{1}{sT_i}+\frac{sT_d}{sT_b+1}\right) \quad (2)$$

where: k_p – the proportional gain, T_i – the integral time, T_d – the derivative time, T_b – the time constant in the derivative part (D) of the controller.

Based on the equations (1) and (2), a simulator of the closed-loop control system was created in LabVIEW environment. The simulator allowed for appropriate choice of the controller structure and for tuning its parameters. Based on the simulation runs, sufficiently good results, i.e., short settling time and no control error, were obtained for the PI (T_d=0) controller with the following parameters: k_p=0.5 and T_i=0.5[s]. A more detailed analysis of the closed-loop system described by (1) and (2) will allow to derive necessary and sufficient conditions for stability of the system. But, in order to determine the stability conditions, at first, it is necessary to find a discrete time description of the closed-loop system. In our case, the input-output description of the closed-loop system is as follows:

$$y(z)\cdot\left(z+k_pk\left(\frac{T}{T_i}\cdot\frac{z}{z-1}+1\right)\right) = w(z)\cdot k_pk\left(\frac{T}{T_i}\cdot\frac{z}{z-1}+1\right) \quad (3)$$

where: y(z), w(z) – are z-transforms of the actual and set point stage position, respectively, k_p – the proportional gain of the controller, T_i – the integral time, k – the gain of the plant and T – the sample time.

Hence, the characteristic equation of the closed-loop system (3) has the following form:

$$z^2\cdot T_i + z\cdot(k_pk\cdot T + k_pk\cdot T_i - T_i) - k_pk\cdot T = 0 \quad (4)$$

The above equation can be easily transformed to Laplace domain by using the well-known relation z:=(s+1)/(s–1). Then, by using the Routh-Hurwitz criterion, the necessary and sufficient condition for stability of (3) is as follows:

$$0 < k_p < \frac{2T_i}{T+2T_i}\cdot\frac{1}{k} \quad (5)$$

The proposed control algorithm was implemented in the control application written in G language in LabVIEW and its front panel is shown in Fig. 5. Owing to the application of ActiveX components provided by the manufacturer of the microactuator, the communication process between the microactuator and the control application is simplified. The information on the microactuator stage position is obtained from the segmented image according to the algorithm described in Section II.

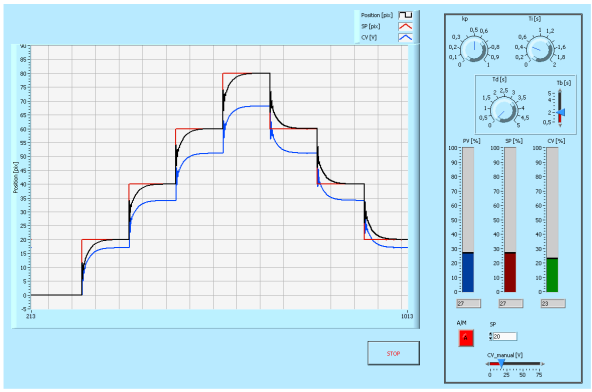

Figure 5. Front panel of the control application in LabVIEW.

Moreover, the implemented algorithm includes the bumpless switching between the automatic and manual modes of operation and the anti-reset windup, i.e., the integral part of the controller is disabled when the upper or lower bound is reached by the control voltage (the controller output signal).

IV. Experimental Results and Concluding Remarks

Fig. 6 presents step responses of the positioning control system for the previously determined structure and parameter values of the PI controller (k_p=0.5, T_i=0.5[s]). The obtained results were compared with step responses of the simulated closed-loop system described by equations (1) and (2) for the same controller parameters.

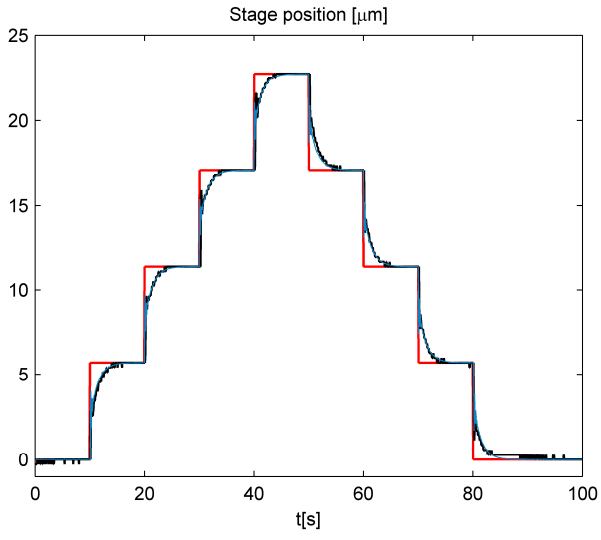

Figure 6. Comparison of the real (black) and simulated (blue) step responses of the closed-loop system. Red line represents changes in the set point position.

Although, there is a good conformity between experimental and simulated positions of the microactuator stage, the

visible differences occur in the transients of control voltages (Fig. 7). Most probably, this is due to the hysteresis effect, which is not included in the description of the simulated plant (1). It is also easy to notice that the hysteresis has an influence on the plant gain, which is dependent on the actual and previous values of the control voltage (Fig. 3).

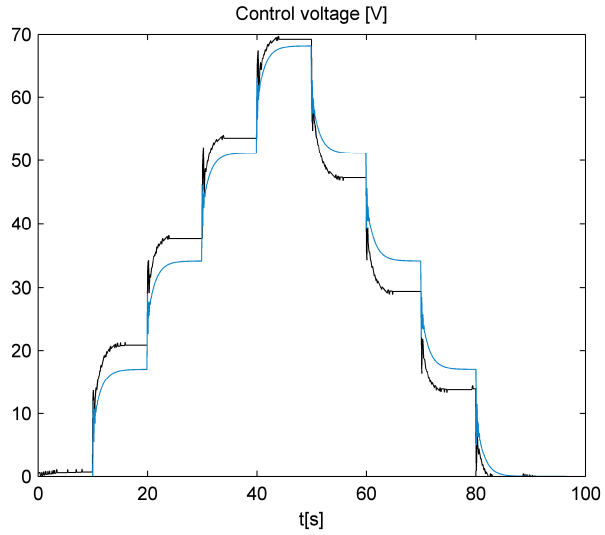

Figure 7. Control voltage in real (black) and simulated (blue) closed-loop control system.

On the other hand, it should be emphasized that the proposed controller ensures a complete elimination of the hysteresis behavior in the relation between the actual and set point stage positions (Fig. 8), which is one of the well-known properties of the closed-loop system.

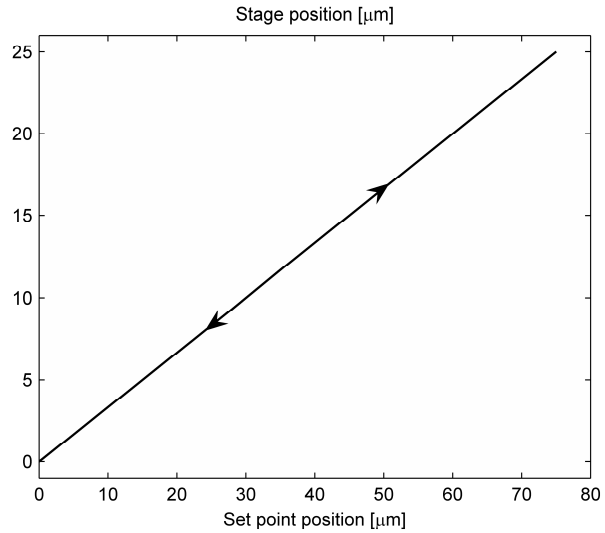

Figure 8. Steady state position in the closed-loop system.

Now, it remains to verify the stability condition (5), which was derived in the previous section for the simplified system (1)-(2). This can be achieved by analyzing the behavior of the positioning control system for large values of the proportional gain k_p (closed to critical values of k_p determined from inequality (5)) and for fixed integral times T_i in the controller. Fig. 9 presents the obtained results on the controller parameter plane (k_p,T_i) and compares the stability regions obtained experimentally and analytically based on the condition (5). In this case, the set point values were changed by 5 to 10 micrometers to cover the whole range of possible displacements of the microactuator stage.

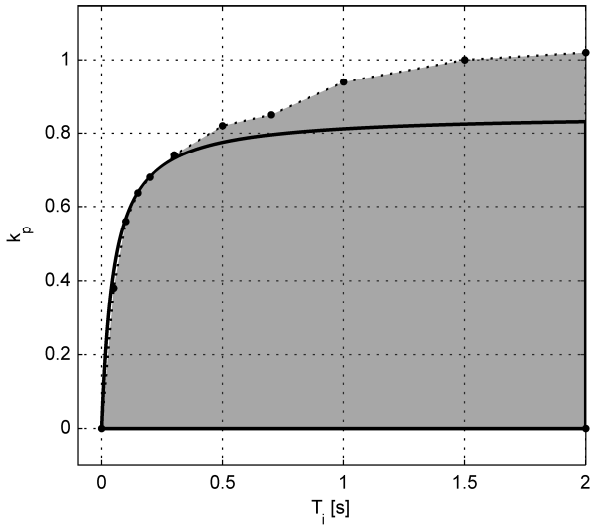

Figure 9. Stability regions of the closed-loop system. Black thick line is a boundary of stability region computed from eqation (5) and black dotted line from experimental results.

The experimental stability region turned out to be larger, than the region resulting from inequality (5). Most probably, the reason for this behavior is due to the hysteresis effect, which is not included in (5). Near the marginal stability boundary, the control voltage changes very rapidly and, as a result, the stage platform moves back and forth at very high frequency. Hence, it is highly probable that the hysteresis plays an important role in the behavior of the positioning control system. However, this should be verified by more detailed analysis. It should also be emphasized that the analytical determination of the stability region is not an easy task for plants, which exhibit hysteresis behavior. On the other hand, if the controller parameters satisfy inequality (5), then the positioning control system is stable.

In conclusion, the presented system allows for positioning of the observed samples with an accuracy of one pixel (several nanometers). It means that the accuracy is dependent on both the resolution of captured image and the total magnification of the optical microscope. At larger magnifications, the graphical indicator will be displaced by a distance of more pixels; hence, one pixel will be corresponding to a smaller distance in nanometers. Similarly, for a fixed magnification, but for a digital camera providing images of higher resolution, there will be more pixels corresponding to the entire range of stage displacement. In effect, the accuracy of positioning will be mainly limited by the current magnification of the optical microscope. The greater the total magnification, the better accuracy of

 ISBN: 978-1-61208-303-2

positioning can be achieved. In the case of using different types of position sensor (e.g., capacitive or strain gauge sensor), the accuracy of positioning control is limited by the accuracy of the applied sensor. Another important issue that must be taken into account in the further development of the system is the speed of positioning of the microactuator stage. In the presented case, acceptable results were obtained by using the classical PI controller. However, to increase the speed of positioning, it is necessary either to tune the controller parameters again without violating the stability condition (5) or to change the structure of controller.

ACKNOWLEDGMENT

This work was supported by the National Science Centre under grant No. 2012/05/B/ST7/00096 and by the Ministry of Science and Higher Education under grant BK-UiUA.

REFERENCES

[1] A. Sinno, P. Ruaux, L. Chassagne, S. Topcu, Y. Alalyli, G. Lerondel, S. Blaize, A. Bruyant, and P. Royer, "Enlarged Sample Holder For Optical AFM Imaging: Millimeter Scanning With High Resolution," First International Conference on Sensor Device Technologies and Applications (SENSORDEVICES 2010), Venice/Mestre, Italy, July 2010, pp. 190–194.

[2] D. Zhang, Z. Gao, M. Malosio, and G. Coppola, "A Novel Flexure Parallel Micromanipulator Based on Multi-Level Displacement Amplifier", The Third International Conference on Sensor Device Technologies and Applications (SENSORDEVICES 2012), Rome, Italy, August 2012, pp. 31–37.

[3] A.J. Fleming, "A review of nanometer resolution position sensors: Operation and performance," Sensor. Actuat. A-Phys., vol. 190, February 2013, pp. 106–126.

[4] S.C. Jordan and P.C. Anthony, "Design Considerations for Micro- and Nanopositioning: Leveraging the Latest for Biophysical Applications," Curr. Pharm. Biotechnol., vol. 10, August 2009, pp. 515–521.

[5] Y-M. Han, S-M. Choi, S-B. Choi, and H-G. Lee, "Design and control of a hybrid mount featuring a magnetorheological fluid and a piezostack," Smart Mater. Struct., vol. 20, July 2011, pp. 1–13.

[6] P-B. Nguyen and S-B Choi, "Micro-position Control of a Piezostack Actuator Using Rate-Dependent Hysteretic Compensator," Int. J. Prec. Eng. Man., vol. 12, October 2011, pp. 885–891.

[7] H.G. Kim, "Nano positioning control for dual stage using minimum order observer," J. Mech. Sci. Technol., vol. 26, March 2012, pp. 941–947.

[8] S.B. Choi, S.R. Hong, and Y.M. Han, "Dynamic characteristics of inertial actuator featuring piezoelectric materials: Experimental verification," J. Sound Vibration, vol. 302, May 2007, pp. 1048–1056.

[9] S.B. Choi, S.S. Han, Y.M. Han, and B.S. Thompson, "A magnification device for precision mechanisms featuring piezoactuators and flexure hinges: Design and experimental validation," Mech. Mach. Theory, vol. 42, September 2007, pp. 1184–1198.

[10] R.J.E. Merry, D.J. Kessels,W.P.M.H. Heemels, M.J.G. van de Molengraft, and M. Steinbuch, "Delay-varying repetitive control with application to a walking piezo actuator," Automatica, vol. 47, August 2011, pp. 1737–1743.

[11] P-B. Nguyen and S-B Choi, "A novel rate-independent hysteresis model of a piezostack actuator using the congruency property," Smart Mater. Struct., vol. 20, May 2011, pp 1–10.

[12] M. De Volder, J. Coosemans, R. Puers, and D. Reynaerts, "Characterization and control of a pneumatic microactuator with an integrated inductive position sensor," Sensor. Actuat. A-Phys., vol. 141, January 2008, pp. 192–200.

[13] P.R. Ouyang, W.J. Zhang, Madan M. Gupta, and W. Zhao, "Overview of the development of a visual based automated bio-micromanipulation system," Mechatronics, vol. 17, December 2007, pp. 578–588.

[14] J. Cas, G. Skorc, and R. Safaric, "Neural network position control of XY piezo actuator stage by visual feedback," Neural. Comput. Applic., vol. 19, October 2010, pp. 1043–1055.

[15] K. Abidi and A. Sabanovic, "Sliding-Mode Control for High-Precision Motion of a Piezostage," IEEE T. Ind. Electron., vol. 54, February 2007, pp. 629–637.

[16] C-Y. Lin and P-Y. Chen, "Precision tracking control of a biaxial piezo stage using repetitive control and double-feedforward compensation," Mechatronics, vol. 21, February 2011, pp. 239–249.

[17] P. Ge and M. Jouaneh, "Modeling hysteresis in piezoceramic actuators," Prec. Eng., vol. 17, July 1995, pp. 211–221.

[18] D. Hughes and J.T.Wen, "Preisach modeling of piezoceramic and shape memory alloy hysteresis," Smart Mater. Struct., vol. 6, June 1997, pp. 287–300.

[19] S.R. Viswamurthy and R. Ganguli, "Modeling and compensation of piezoceramic actuator hysteresis for helicopter vibration control," Sensor. Actuat. A-Phys., vol. 135, April 2007, pp. 801–810.

[20] L. Deng and Y. Tan, "Modeling hysteresis in piezoelectric actuators using NARMAX models," Sensor. Actuat. A-Phys., vol. 149, January 2009, pp. 106–112.

[21] M. Kinouchi, I. Hayashi, N. Iwatsuki, K. Morikawa, J. Shibata, and K. Suzuki, "Application of Fuzzy PI control to improve the positioning accuracy of a rotary-linear motor driven by two-dimensional ultrasonic actuators," Microprocess. Microsyst., vol. 24, April 2000, pp. 105–112.

[22] F. Preisach, "Über die magnetische Nachwirkung," Z. Phys., vol. 94, May 1935, pp. 277–302.

[23] I.D. Mayergoyz and G. Friedman, "Generalized Preisach model of hysteresis". IEEE T. Magn., vol. 24, January 1988, pp. 212–217.

[24] L. Chuntaoa and T. Yonghong, "A neural networks model for hysteresis nonlinearity", Sensor. Actuat. A-Phys., vol. 112, April 2004, pp. 49–54.

 ISBN: 978-1-61208-303-2